ACS NANO

www.acsnano.org

LETTER TO THE EDITOR

Letter to the Editor Concerning "Simultaneous, Single-Particle Measurements of Size and Loading Give Insights into the Structure of Drug-Delivery Nanoparticles"

Andrew C. Madison,[⊥] Adam L. Pintar,[⊥] Craig R. Copeland, Natalia Farkas, and Samuel M. Stavis*

Cite This: *ACS Nano* 2023, 17, 8837−8842

Read Online

ACCESS | Metrics & More | Article Recommendations | Supporting Information

The vexing error of excess variance in measurements of nanoparticle size distributions degrades accuracy in applications ranging from quality control of nanoparticle products to hazard assessment of nanoplastic byproducts. The particular importance of lipid nanoparticles for vaccine and medicine delivery motivates this Letter to the Editor, which concerns a publication[1] in *ACS Nano* and also presents original research. In ref 1, the benchmark measurements of a nanoparticle standard manifest large errors of the size distribution that contradict the claim of validation. In subsequent applications of the method to measure lipid nanoparticles, potential errors could bias the correlation of fluorescence intensity as an optical proxy for molecular loading and give misleading insights from power-law models of intensity−size trends. Looking forward, measurement error models may address this issue.

A brief review provides helpful context. Heterogeneous sizes and properties of colloidal nanoparticles are challenging to measure. Measurements of nanoparticle ensembles often cannot resolve size and property distributions, providing only estimates of means——ordinarily arithmetic means but occasionally harmonic means——and variances. For example, photon correlation spectroscopy or dynamic light scattering,[2] which is in common use and abuse for measuring these values,[3] as well as fluorescence correlation spectroscopy,[4] which contends with focal volume artifacts,[5] rearrange the Stokes−Einstein−Sutherland[6,7] equation to infer hydrodynamic diameter from ensemble diffusivity. Ensemble measurements can output some information about the molecular loading of lipid nanoparticles if size distributions are available as additional inputs,[8] but measurements of single nanoparticles can be more informative and less dependent on model assumptions. Nanoparticle tracking analysis,[9] which is the basis of the measurement method in ref 1, infers the hydrodynamic diameters of single nanoparticles from optical microscopy of diffusive trajectories, and also yields estimates of optical properties such as fluorescence intensity for correlation. However, short trajectories through the focal volume of an optical microscope limit sizing resolution, motivating Bayesian statistical analyses to improve accuracy[10] and fluidic devices to confine nanoparticles, prolong tracking, and improve sizing resolution.[11]

Measurement Function. A consequence of fluidic confinement is a reduction of nanoparticle diffusivity through hydrodynamic interactions, requiring a correction for this systematic effect. In the simplest case of a confining slit, the resulting measurement function is

$$d_h = \frac{k_B}{3\pi} \cdot \frac{T}{\eta} \cdot \frac{C}{D_{||}} \tag{1}$$

where d_h is the hydrodynamic diameter of a single nanoparticle, k_B is the Boltzmann constant, T is the absolute temperature of the dispersion fluid, η is the kinematic viscosity of the dispersion fluid, C is a hydrodynamic correction, and $D_{||}$ is the diffusivity parallel to the slit surfaces (Table S1). In ref 1

$$C \approx \left(1 - 1.004\left(\frac{d_h}{d_s}\right) + 0.418\left(\frac{d_h}{d_s}\right)^3 + 0.210\left(\frac{d_h}{d_s}\right)^4 - 0.169\left(\frac{d_h}{d_s}\right)^5\right) \tag{2}$$

where d_s is the slit depth.[12,13]

Input Quantities. The measurement function in eq 1 has multiple input quantities that require consideration and that can introduce systematic effects, whereas ref 1 reports only nominal values of d_s and apparent values of $D_{||}$. Regarding T/η, quantitation of fluid temperature and viscosity, and validation of temperature stability and fluid quiescence, are all necessary but absent from ref 1. Regarding $C/D_{||}$, the hydrodynamic correction[12,13] applies only at the midplane of a slit and deviates significantly from the results of careful measurements of microparticle diffusion near the surface of a slit,[14] and a mean correction neglects the varying diameters of single nanoparticles. Further, the analysis in ref 1 extracts $D_{||}$ from a

Received: May 18, 2022
Revised: March 20, 2023
Accepted: April 26, 2023
Published: May 23, 2023

Table 1. Data from Table 2 of Reference 1 and Figure 1F of Reference 1[a]

property	source	quantity (nm)				
microwell depth	Table 2	**200**	**350**	**500**	**800**	**1200**
particle size from mean diffusivity	Table 2	62 ± 2	45 ± 2	47 ± 1	48 ± 2	43 ± 1
harmonic mean diameter	Figure 1F	61.3 ± 2.5	46.8 ± 1.0	48.6 ± 0.7	48.2 ± 0.8	45.3 ± 1.2
arithmetic mean diameter	Figure 1F	73.1 ± 3.2	52.9 ± 1.0	52.8 ± 0.8	52.2 ± 0.8	50.8 ± 1.3
standard deviation of diameter	Figure 1F	33.9 ± 3.6	18.6 ± 0.7	15.9 ± 0.6	14.7 ± 0.6	18.3 ± 1.0

[a]Bold text indicates data from Table 2 of ref 1. Regular text indicates new analysis of Figure 1F of ref 1. Uncertainties therein are 68% coverage intervals of digitizing errors and sampling variability (Supporting Information, Notes S1–S3 of this Letter).

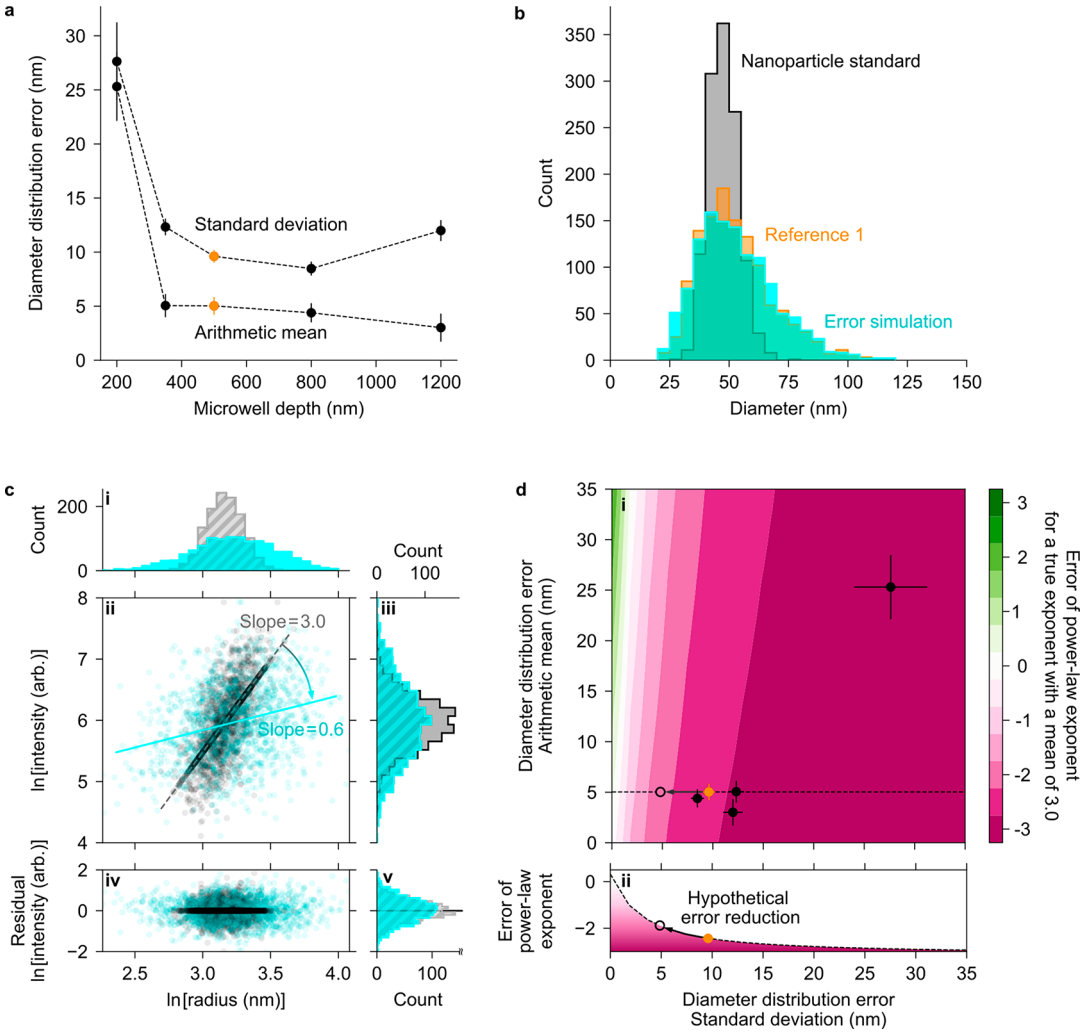

Figure 1. (a) Scatter plot showing diameter distribution errors from the benchmark measurements of a nanoparticle standard in ref 1. Vertical bars are 68% coverage intervals of digitizing errors and sampling variability (Supporting Information of this Letter). (b) Histograms showing representative diameter distributions of (gray) the nanoparticle standard, (orange) ref 1, for the corresponding orange data marker in (a), and (cyan) an error simulation. (c) Marginal histograms and scatter plots showing a representative negative bias that is evident as a slope suppression in a linear model of ln (intensity) versus ln (radius). (c-i,iii) (Solid gray with black outline) Marginal histograms showing reference data without measurement errors. (Hatch gray with gray outline) Marginal histograms showing data with ln (intensity) errors only. (Solid cyan) Marginal histograms showing data with both ln (intensity) and ln (radius) errors. (c-ii) Scatter plots showing ln (intensity) versus ln (radius) data (black data markers) without measurement errors, (gray data markers) with ln (intensity) errors, and (cyan data markers) with both ln (intensity) and ln (radius) errors. (Dash gray) Line showing least-squares fit to gray data markers. (Solid cyan) Line showing least-squares fit to cyan data markers. (c-i,v) Scatter plot and marginal histograms showing residual values of ln (intensity) from the fits in (c-ii), with approximately normal distributions around means of zero. (d-i,ii) Contour plot and (dash section) line plot showing errors of the power-law exponent for a true exponent with a representative mean of 3.0 in a factorial analysis as a function of diameter distribution errors. The five data markers in (d-i) correspond to the five microwell depths in (a). Uncertainty of the error of the power-law exponent in (d-ii) is smaller than the orange data marker. The black arrow and open circle correspond to a hypothetical halving of a representative error of the standard deviation between the efforts to validate and apply the measurement method.

model of diffusion in two dimensions in a confining circle,[15] whereas C corrects the parallel component of diffusion in three dimensions in a confining slit. Neither aspect matches the experimental scheme of diffusion in a confining cylinder, and a

https://doi.org/10.1021/acsnano.2c04894
ACS Nano 2023, 17, 8837–8842

representative model fit systematically underestimates the experimental data at short lag times (Figure 1D of ref 1). As well, optical microscopy throughout a wide[16] and deep[17] focal volume requires calibration of scale factor and aberration artifacts such as distortion and defocus to correct apparent trajectories that are the source data for $D_{\|}$. Finally, a formal measurement requires accurate estimates of not only input quantities but also input uncertainties, and their propagation through the measurement function to an output quantity and output uncertainty,[18] which is incomplete in ref 1.

Nanoparticle Standard. Even after a complete evaluation of uncertainty, independent validation is necessary. The effort to validate in ref 1 involves tests of a nanoparticle standard, consisting of polystyrene spheres loaded with hydrophobic fluorophores, in cylindrical microwells of five depths (Table 1 of this Letter). Validation would require agreement of the test results with at least two reference values of the diameter distribution—a mean of 47.8 ± 0.3 nm and a root variance or standard deviation of 6.3 ± 0.2 nm.[19] These uncertainties are 68% coverage intervals of sampling variability only, neglecting potential uncertainty from other sources. Moreover, the experimental measurement method of ref 1 yields a hydrodynamic size, diverging from the reference measurement method of transmission electron microscopy,[19,20] which yields a steric size. Setting aside this divergence, this key comparison suffices to critically evaluate the foundational claim of ref 1—validation of the measurement method by agreement with the expected size within ±1 nm. In a primary aspect of experimental design that follows from the basic purpose of method validation, the nanoparticle standard in ref 1 was chosen to match the diameter of lipid nanoparticles in subsequent applications of the measurement method.

Fitting Analysis. Reference 1 involves sizing of single nanoparticles but also aspects of ensemble analysis. Reference 1 claims that the histograms in Figure 1F show the collapse of different diffusivity distributions onto the same size distribution after hydrodynamic correction, excluding data from the shallowest device. Yet, the analysis in ref 1 calculates the mean diffusivity for each microwell depth and fits the hydrodynamic correction to all of the data, including data from the shallowest device, reporting a peak diameter of 49 ± 6 nm. This value of fit uncertainty is distinct from the reference value of standard deviation—the two values are only coincidentally equal, as the following subsection of this Letter on distributional errors shows. The fitting analysis in ref 1, or alternatively combining the diameter histograms after hydrodynamic correction, could cause random effects to cancel, as would occur for replicate measurements. However, several of the systematic effects depend on microwell depth, and an assumption that they should cancel would be questionable.

Independent Analysis. This issue motivates a new analysis for each microwell depth independently (Table 1 of this Letter), which assumes nothing of the correctness of fitting or combining all of the data, and yields two root-mean-square errors as conventional metrics of accuracy. This analysis involves data from all five microwell depths, matching the effort to validate, as well as one of the three applications of the method to measure lipid nanoparticles in ref 1. The analysis begins with calculation of the harmonic mean, arithmetic mean, and standard deviation of each diameter histogram in Figure 1F of ref 1 (Supporting Information, Tables S2−S7 and Notes S1−S3 of this Letter).[21,22] The nanoparticle sizes from mean diffusivity in Table 2 of ref 1 and the harmonic mean diameters agree within uncertainty, which is consistent with the inverse proportionality of arithmetic mean diffusivity and harmonic mean diameter in the Stokes−Einstein−Sutherland equation. A similar effect results from ensemble averaging in dynamic light scattering,[3] building confidence in the new analysis. However, the analysis in ref 1 overlooks this relation, resulting in a critical inconsistency—the key comparison to the reference values requires the arithmetic means, rather than the harmonic means, as well as the standard deviations of the diameter distributions.

Distributional Errors. All of the arithmetic mean diameters exceed the reference value of 47.8 ± 0.3 nm (Figure 1a of this Letter), yielding a root-mean-square error of 12.0 nm or 25.1%. This error is an order of magnitude greater than the corresponding claim of ref 1, confirming the presence of systematic effects. The standard deviations of diameter are even more problematic. Reference 1 acknowledges excess variance due to short trajectories from fluorescence photobleaching but avoids quantifying the distribution widths. All of the standard deviations of diameter exceed the reference value of 6.3 ± 0.2 nm (Figure 1a of this Letter), yielding a root-mean square error of 15.6 nm or 247%. This large error corresponds to diameter histograms that are several times wider than the reference diameter distribution, showing low resolution for sizing single nanoparticles. On this basis, the claim of validation of the measurement method by agreement with the expected size within ±1 nm lacks substantiation.

Experimental Disconnect. In the subsequent applications of the measurement method in ref 1, a different objective lens and imaging conditions prolong the tracking analysis from 600 to 2000 images. Although longer trajectories could reduce the error of the standard deviation[11] by up to a factor of $\sqrt{2000/600} = 1.83 \approx 2$, different systematic effects could also be present due to scale factor and aberration artifacts that are intrinsic to objective lenses.[16,17] As well, ref 1 notes potential errors due to a hard-sphere analysis of soft-lipid nanoparticles with complex diffusive behavior. This mismatch of experimental conditions and potential errors disconnects the efforts to validate and apply the measurement method.

Potential Bias. This disconnect results in uncertain sizing errors in applications of the measurement method. However, even allowing for a hypothetical halving of the error of the standard deviation, a potential bias[23] raises a question about the reliability of the results. A major goal of ref 1 is to use power-law models of the dependence of fluorescence intensity on hydrodynamic size to study the loading of fluorophores into lipid nanoparticles. In ordinary least-squares fits of such data, unrecognized errors of the independent variable of size can bias estimated parameters of models of the dependent variable of intensity.[23] The potential bias depends on the widths of both the true and measurement error distributions of the independent variable[24] and becomes critical in comparisons of expected and observed power-law exponents, which guide interpretation of the results in ref 1. Reference 1 omits such analysis for the standard, which presents another opportunity to test expectations against observations, given sufficient sizing resolution.[25,26]

Size Simulations. Monte Carlo simulations elucidate the potential bias for the reference diameter and sizing error distributions in ref 1 (Supporting Information, Notes S4 of this Letter), whereas both distributions are uncertain for the lipid nanoparticles. Without access to a reference diameter histogram for the nanoparticle standard, the reference mean and

https://doi.org/10.1021/acsnano.2c04894
ACS Nano 2023, 17, 8837−8842

standard deviation parametrize a log-normal distribution of diameter, d. This common model allows characteristic asymmetry of nanoparticle size distributions.[27,28] A symmetric normal distribution yields similar results (Supporting Information of this Letter). Skew-normal distributions of diameter errors approximate unknown combinations of random and systematic effects in ref 1, with model parameters resulting from deconvolution of the experimental histograms in Figure 1 of ref 1 with the reference diameter distribution. This new analysis yields synthetic histograms that closely match the experimental histograms in Figure 1F of ref 1 (Figure 1b, Supporting Information, Figure S1 of this Letter). Per the choice of the standard and the effort to validate, these histograms should resemble the diameter histograms of lipid nanoparticles in Figures 2, 3, and 6 of ref 1.

Intensity Simulations. A power law then constrains fluorescence intensity, I, by the model, $I = \gamma r^{\beta}$, with a coefficient, γ, an exponent, β, and changing the independent variable from diameter d to radius r, as in ref 1. A transformation of this model by the natural logarithm, $\ln(I) = \beta \ln(r) + \ln(\gamma)$, serves three purposes. First, this transformation facilitates modeling of ln (intensity) errors by a normal distribution with a mean of zero and a range of standard deviations that approximate the vertical scatter of ln (intensity) values at the central radii in Figures 2, 3, and 6 of ref 1, capturing both measurement variability and sample heterogeneity (Figure 1c, Supporting Information, Figure S2 and Table S8 of this Letter). Second, this transformation enables ordinary least-squares fits of linear models to the ln (intensity) versus ln (radius) data, with the slope β equaling the power-law exponent, as in Figure 6 of ref 1. Third, this transformation facilitates a comparison to the canonical example of slope suppression that motivates a measurement error model.[23]

Slope Suppression. A factorial study shows that the predominant effect is a suppression of the slope by the error of the standard deviation of the diameter distribution (Figure 1c, Supporting Information, Figures S2 and S3 of this Letter). This study considers true slopes ranging from 1.5 to 3.5, with a value of 3.0 matching the upper limit expected in ref 1. This negative bias has an intuitive explanation—excess variance increases the run of ln (radius) for a constant rise of ln (intensity), reducing the slope of the trend. This slope, which is equivalent to the exponent of a power-law model, nominally gives physical or chemical insight, such as by the proportionality of fluorophore count to loading processes that depend on surface area or volume. Accordingly, this bias of the power-law exponent can give misleading insights, potentially confounding intensity−size correlation in ref 1. For the range of distributional errors in the effort to validate in ref 1, errors of the arithmetic mean that are much larger than errors of the standard deviation can cancel this bias (Figure 1d of this Letter). However, the distributional errors in the effort to validate have the opposite relation, indicating that the results lie outside of this cancellation band, even allowing for a hypothetical halving of the error of the standard deviation between efforts to validate and apply the measurement method (Figure 1d of this Letter). Moreover, even if a cancellation of errors were to occur in applications of the measurement method, this would constitute an unreliable basis for an accurate measurement, substantiating the question of reliability.

Conclusion. The scope of ref 1 is ambitious, the experiments are challenging, and the effort of the authors is commendable. However, a distributional validation is necessary to fairly compare and reliably apply methods to measure single nanoparticles. Agreement of both the mean and the standard deviation of a nanoparticle size distribution near the scale of 1 nm requires comprehensive calibration and reveals the potential for unexpectedly high power-law exponents modeling intensity−size trends, even for the common standards benchmarked in ref 1.[25,26] An answer to the question of the reliability of the power-law exponents in ref 1 would require quantitative analysis of both the true and sizing error distributions of lipid nanoparticle diameters. However, the susceptibility of such exponents to suppression by sizing errors of the standard deviation presents a surprising possibility—observation of an expected exponent, which would ordinarily build confidence, could instead result from a biased measurement of an unexpectedly high exponent. For this reason, accurate measurements, rather than hypothetical expectations of fluorophore loading trends that neglect the full scope of interactions of light with dielectric nanostructures, are necessary to support reliable studies of lipid nanoparticles for vaccine and medicine delivery, as well as studies that involve nanoplastic standards for hazard assessment. Even so, in these[25,26] and other[29,30] studies, any sizing error is of concern. This Letter to the Editor not only identifies this problem but also proposes a potential solution by the deconvolution of experimental histograms with reference histograms to inform measurement error models.[23] Future studies may benefit from the use of such models to avoid biases in property correlation and parameter estimation.

ASSOCIATED CONTENT

Supporting Information

The Supporting Information is available free of charge at https://pubs.acs.org/doi/10.1021/acsnano.2c04894.

Terminology; arithmetic and harmonic means; diameter histograms; histogram digitization; digitization uncertainty; bin data; error modeling and simulation; computational deconvolution; simulation parameters; slope suppression; average effects (PDF)

AUTHOR INFORMATION

Corresponding Author

Samuel M. Stavis − *Microsystems and Nanotechnology Division, National Institute of Standards and Technology, Gaithersburg, Maryland 20899, United States;* orcid.org/0000-0002-7108-1405; Email: sstavis@nist.gov

Authors

Andrew C. Madison − *Microsystems and Nanotechnology Division, National Institute of Standards and Technology, Gaithersburg, Maryland 20899, United States;* orcid.org/0000-0002-9456-2754

Adam L. Pintar − *Statistical Engineering Division, National Institute of Standards and Technology, Gaithersburg, Maryland 20899, United States;* orcid.org/0000-0002-5021-2576

Craig R. Copeland − *Microsystems and Nanotechnology Division, National Institute of Standards and Technology, Gaithersburg, Maryland 20899, United States;* orcid.org/0000-0002-3340-0006

https://doi.org/10.1021/acsnano.2c04894
ACS Nano 2023, 17, 8837−8842

Natalia Farkas − *Microsystems and Nanotechnology Division, National Institute of Standards and Technology, Gaithersburg, Maryland 20899, United States; Theiss Research, La Jolla, California 92037, United States; Building and Fire Sciences, United States Forest Service, Forest Products Laboratory, Madison, Wisconsin 53726, United States;* orcid.org/0000-0002-7102-7345

Complete contact information is available at: https://pubs.acs.org/10.1021/acsnano.2c04894

Author Contributions

⊥A.C.M. and A.L.P. made equal contributions.

Notes

The identification of a commercial product in ref 19 is for specification only and does not imply recommendation. This Letter to the Editor has an associated preprint: Madison, A. C.; Pintar, A. L.; Copeland, C. R.; Farkas, N.; Stavis, S. M. Letter to the Editor Concerning Simultaneous, Single-Particle Measurements of Size and Loading Give Insights into the Structure of Drug-Delivery Nanoparticles. *arXiv* 2023, arXiv:2302.01778; https://arxiv.org/abs/2302.01778 (accessed March 20, 2023).

ACKNOWLEDGMENTS

The authors gratefully acknowledge an anonymous reviewer, J. Fagan, J. A. Liddle, J. Kramar, and E. A. Strychalski for helpful comments, and the National Institute of Standards and Technology Strategic and Emerging Research Initiative in support of the Circular Economy Program.

REFERENCES

(1) Kamanzi, A.; Gu, Y.; Tahvildari, R.; Friedenberger, Z.; Zhu, X.; Berti, R.; Kurylowicz, M.; Witzigmann, D.; Kulkarni, J. A.; Leung, J.; Andersson, J.; Dahlin, A.; Höök, F.; Sutton, M.; Cullis, P. R.; Leslie, S. Simultaneous, Single-Particle Measurements of Size and Loading Give Insights into the Structure of Drug-Delivery Nanoparticles. *ACS Nano* **2021**, *15* (12), 19244−19255.

(2) Foord, R.; Jakeman, E.; Oliver, C. J.; Pike, E. R.; Blagrove, R. J.; Wood, E.; Peacocke, A. R. Determination of Diffusion Coefficients of Haemocyanin at Low Concentration by Intensity Fluctuation Spectroscopy of Scattered Laser Light. *Nature* **1970**, *227* (5255), 242−245.

(3) Farkas, N.; Kramar, J. A. Dynamic light scattering distributions by any means. *J. Nanopart. Res.* **2021**, *23* (5), 120.

(4) Magde, D.; Elson, E. L.; Webb, W. W. Fluorescence correlation spectroscopy. II. An experimental realization. *Biopolymers* **1974**, *13* (1), 29−61.

(5) Hess, S. T.; Webb, W. W. Focal volume optics and experimental artifacts in confocal fluorescence correlation spectroscopy. *Biophys. J.* **2002**, *83* (4), 2300−2317.

(6) Einstein, A. Über die von der molekularkinetischen Theorie der Wärme geforderte Bewegung von in ruhenden Flüssigkeiten suspendierten Teilche. *Annalen der Physik* **1905**, *322* (8), 549−560.

(7) Sutherland, W. A dynamical theory of diffusion for non-electrolytes and the molecular mass of albumin. *London, Edinburgh, and Dublin Philosophical Magazine and Journal of Science* **1905**, *9* (54), 781−785.

(8) Reiner, J. E.; Jahn, A.; Stavis, S. M.; Culbertson, M. J.; Vreeland, W. N.; Burden, D. L.; Geist, J.; Gaitan, M. Accurate Optical Analysis of Single-Molecule Entrapment in Nanoscale Vesicles. *Anal. Chem.* **2010**, *82* (1), 180−188.

(9) Filipe, V.; Hawe, A.; Jiskoot, W. Critical Evaluation of Nanoparticle Tracking Analysis (NTA) by NanoSight for the Measurement of Nanoparticles and Protein Aggregates. *Pharm. Res.* **2010**, *27* (5), 796−810.

(10) Silmore, K. S.; Gong, X.; Strano, M. S.; Swan, J. W. High-Resolution Nanoparticle Sizing with Maximum A Posteriori Nanoparticle Tracking Analysis. *ACS Nano* **2019**, *13* (4), 3940−3952.

(11) Haiden, C.; Wopelka, T.; Jech, M.; Keplinger, F.; Vellekoop, M. J. Sizing of Metallic Nanoparticles Confined to a Microfluidic Film Applying Dark-Field Particle Tracking. *Langmuir* **2014**, *30* (31), 9607−9615.

(12) Faxén, H. Der Widerstand gegen die Bewegung einer starren Kugel in einer zähen Flüssigkeit, die zwischen zwei parallelen ebenen Wänden eingeschlossen ist. *Annalen der Physik* **1922**, *373* (10), 89−119.

(13) Happel, J.; Brenner, H. Low Reynolds number hydrodynamics: with special applications to particulate media. *Mechanics of Fluids and Transport Processes*; Springer: Dordrecht, The Netherlands; 1983; Vol. *1*, DOI: 10.1007/978-94-009-8352-6.

(14) Lin, B.; Yu, J.; Rice, S. A. Direct measurements of constrained Brownian motion of an isolated sphere between two walls. *Phys. Rev. E* **2000**, *62* (3), 3909−3919.

(15) Bickel, T. A note on confined diffusion. *Physica A: Statistical Mechanics and its Applications* **2007**, *377* (1), 24−32.

(16) Copeland, C. R.; Geist, J.; McGray, C. D.; Aksyuk, V. A.; Liddle, J. A.; Ilic, B. R.; Stavis, S. M. Subnanometer localization accuracy in widefield optical microscopy. *Light: Science & Applications* **2018**, *7* (1), 31.

(17) Copeland, C. R.; McGray, C. D.; Ilic, B. R.; Geist, J.; Stavis, S. M. Accurate localization microscopy by intrinsic aberration calibration. *Nat. Commun.* **2021**, *12* (1), 3925.

(18) Possolo, A. Simple Guide for Evaluating and Expressing the Uncertainty of NIST Measurement Results. *NIST Technical Note 1900*, 2015.

(19) Life Technologies. *Product F-10720, Component A, Lot 1241418*, 2012.

(20) Phillips, S. D.; Estler, W. T.; Doiron, T.; Eberhardt, K.; Levenson, M. A careful consideration of the calibration concept. *Journal of Research of the National Institute of Standards and Technology* **2001**, *106* (2), 371.

(21) *WebPlotDigitizer Version 4.5*; August 2021; https://automeris.io/WebPlotDigitizer (accessed March 11, 2022).

(22) Drevon, D.; Fursa, S. R.; Malcolm, A. L. Intercoder Reliability and Validity of WebPlotDigitizer in Extracting Graphed Data. *Behavior Modification* **2017**, *41* (2), 323−339.

(23) Fuller, W. A. *Measurement Error Models*; Wiley, 2009.

(24) Chen, X.; Hong, H.; Nekipelov, D. Measurement error models. *Prepared for the Journal of Economic Literature* **2007**, https://web.stanford.edu/~doubleh/eco273B/survey-jan27chenhandenis-07.pdf (accessed March 20, 2023).

(25) Liao, K.-T.; Madison, A. C.; Pintar, A. L.; Ilic, B. R.; Copeland, C. R.; Stavis, S. M. A lateral nanoflow assay reveals surprising nanoplastic fluorescence. *arXiv 2101.03881* **2020**, https://doi.org/10.48550/arXiv.2101.03881 (accessed March 20, 2023).

(26) Liao, K.-T.; Schumacher, J.; Lezec, H. J.; Stavis, S. M. Subnanometer structure and function from ion beams through complex fluidics to fluorescent particles. *Lab Chip* **2018**, *18* (1), 139−152.

(27) Limpert, E.; Stahel, W. A.; Abbt, M. Log-normal distributions across the sciences: keys and clues: on the charms of statistics, and how mechanical models resembling gambling machines offer a link to a handy way to characterize log-normal distributions, which can provide deeper insight into variability and probability—normal or log-normal: that is the question. *BioScience* **2001**, *51* (5), 341−352.

(28) Stavis, S. M.; Fagan, J. A.; Stopa, M.; Liddle, J. A. Nanoparticle Manufacturing - Heterogeneity through Processes to Products. *ACS Applied Nano Materials* **2018**, *1* (9), 4358−4385.

(29) Block, S.; Fast, B. J.; Lundgren, A.; Zhdanov, V. P.; Höök, F. Two-dimensional flow nanometry of biological nanoparticles for accurate determination of their size and emission intensity. *Nat. Commun.* **2016**, *7* (1), 12956.

(30) Molenaar, R.; Chatterjee, S.; Kamphuis, B.; Segers-Nolten, I. M.; Claessens, M. M.; Blum, C. Nanoplastic sizes and numbers:

quantification by single particle tracking. *Environmental Science: Nano* **2021**, *8* (3), 723−730.

https://doi.org/10.1021/acsnano.2c04894
ACS Nano 2023, 17, 8837−8842